

Development of Rift valley fever encephalitis in rats is mediated by early infection of olfactory epithelium and neuroinvasion across the cribriform plate

Devin A. Boyles^{1†}, Madeline M. Schwarz^{1,2†}, Joseph R. Albe¹, Cynthia M. McMillen^{1,2}, Katherine J. O'Malley¹, Douglas S. Reed^{1,3} and Amy L. Hartman^{1,2,*}

Abstract

The zoonotic emerging Rift Valley fever virus (RVFV) causes sporadic disease in livestock and humans throughout Africa and the Saudi Arabian peninsula. Infection of people with RVFV can occur through mosquito bite or mucosal exposure during butchering or milking of infected livestock. Disease typically presents as a self-limiting fever; however, in rare cases, hepatitis, encephalitis and ocular disease may occur. Recent studies have illuminated the neuropathogenic mechanisms of RVFV in a rat aerosol infection model. Neurological disease in rats is characterized by breakdown of the blood–brain barrier late in infection, infiltration of leukocytes to the central nervous system (CNS) and massive viral replication in the brain. However, the route of RVFV entry into the CNS after inhalational exposure remains unknown. Here, we visualized the entire nasal olfactory route from snout to brain after RVFV infection using RNA *in situ* hybridization and immunofluorescence microscopy. We found widespread RVFV-infected cells within the olfactory epithelium, across the cribriform plate, and in the glomerular region of the olfactory bulb within 2 days of infection. These results indicate that the olfactory tract is a major route of infection of the brain after inhalational exposure. A better understanding of potential neuroinvasion pathways can support the design of more effective therapeutic regimens for the treatment of neurological disease caused by RVFV.

INTRODUCTION

Rift Valley fever virus (RVFV) is an emerging mosquito-borne zoonotic pathogen that is endemic to Africa and the Middle East, where it infects domestic ruminants and causes fatal hepatic necrosis and ‘abortion storms’ amongst livestock herds [1]. Humans can be infected via mosquito bite, or from mucosal exposure and/or inhalation of infectious particles from affected livestock [1]. Infected people typically experience a self-limiting febrile illness that, in 1–2% of cases, can advance to haemorrhagic fever, hepatitis, neurological disease, or ocular disease [2–4]. In patients that develop encephalitis, there is a 50% chance of death, while survivors can experience long-term neurological complications [5].

Individuals with ocular lesions may experience permanent blindness [3, 5, 6]. Tissue samples from human autopsies are limited and show brain lesions, neuronal death and inflammation within the central nervous system (CNS) [7]. Animal workers such as farmers, veterinarians and butchers are at high risk for mucosal or respiratory exposure and more severe clinical outcomes from RVFV [8–11].

There is a significant risk of death and morbidity in the event that RVF progresses to neurological disease, and not much is known about the pathogenic mechanisms of RVF encephalitis compared to the more extensively studied hepatic disease. In several animal models, respiratory infection by intranasal or aerosol exposure is more likely to lead to encephalitis than

Received 16 September 2020; Accepted 30 October 2020; Published 24 November 2020

Author affiliations: ¹Center for Vaccine Research, University of Pittsburgh, Pittsburgh, PA, USA; ²Department of Infectious Diseases and Microbiology, University of Pittsburgh, Pittsburgh, PA, USA; ³Department of Immunology, University of Pittsburgh, Pittsburgh, PA, USA.

*Correspondence: Amy L. Hartman, hartman2@pitt.edu

Keywords: aerosol; cribriform plate; encephalitis; olfactory bulb; pathogenesis; Rift Valley fever virus.

Abbreviations: BBB, blood brain barrier; BSC, biosafety cabinet; BSL-3, biosafety level 3; CDC, Centers for Disease Control; CNS, Central nervous system; CTL, control; DMEM, Dulbecco's modified eagle's media; FBS, fetal bovine serum; FSAP, Federal Select Agent Program; GL, glomerular layer; IHC, immunohistochemistry; ISH, *in situ* hybridization; LACV, La Crosse virus; LD50, lethal dose 50%; NHP, non human primate; OB, olfactory bulb; OE, olfactory epithelium; ORN, olfactory receptor neuron; PAPR, powered air purifying respirator; PBS, phosphate buffered saline; PFA, paraformaldehyde; PG, periglomerular; PVA, polyvinyl alcohol; RBL, regional biocontainment laboratory; RT, room temperature; RVFV, Rift Valley fever virus; SIV, simian immunodeficiency virus; vRNA, viral RNA.

†These authors contributed equally to this work

001522 © 2021 The Authors



This is an open-access article distributed under the terms of the Creative Commons Attribution License.

peripheral infection routes [12–18]. Our previous studies have characterized the Lewis rat model of RVFV encephalitis, in which rats exposed to aerosolized RVFV succumb to meningoencephalitis within 7–8 days post-infection (p.i.) [19, 20]. By 1 day p.i., viral RNA (vRNA) can be detected at low levels in the brain along with a transient inflammatory leukocyte infiltration [19, 20]. The later stages of disease (5–7 days p.i.) are characterized by blood–brain barrier (BBB) breakdown, an influx of neutrophils, high levels of infectious virus replicating in the brain and extensive neuronal necrosis, which is similar to the histological observations made in human patient samples [5, 7, 21]. Rats become symptomatic by 5–7 days p.i. with fever, weight loss, ruffled fur, hunched posture, porphyrin staining and erratic behavioural manifestations, such as cage circling, horizontal rolling, head tilting and tremors [19].

Despite increased knowledge about the pathogenic mechanisms leading to RVFV encephalitis in animal models, the route of initial CNS invasion has not been elucidated in the rat model. The presence of early leukocytes and low levels of vRNA in the brain at 1–2 days p.i. suggests that the virus enters the brain before widescale vascular breakdown occurs much later in infection (5–6 days p.i.) [20]. The olfactory system presents a potential avenue of CNS invasion for pathogens entering the upper respiratory tract. Olfactory receptor neurons (ORNs) are ciliated, bipolar cells residing within the

olfactory epithelium (OE). Dendrites of ORNs project into the surface of the OE, whereas the axons of ORNs span into the lamina propria, extend through channels in the cribriform plate and attach to the glomerular layer within the olfactory bulb (OB) of the brain (Fig. 1). The earliest appearance of RVFV vRNA in this region at 1–2 days p.i. suggests the ability of the virus to either directly infect ORNs (as seen with herpes simplex type-1 virus [22, 23] and Nipah virus [24]) or to travel through neuron unsheathing cell channels (as, potentially, seen in La Crosse virus infection [25]). Other neuroinvasion mechanisms, such as haematogenous entry via the BBB (as seen with Epstein–Barr virus [26]), ‘trojan horse’ entry into the BBB via infection of monocytes (as seen in simian immunodeficiency virus infection [27]), or travel through neuromuscular junctions (as seen with poliovirus [28, 29]), are less likely. The direct connection between the olfactory neurons and the OB is short, and channels formed between individual olfactory neurons can fit particles up to 100 nm. Bunyaviruses, which are 90 to 100 nm in diameter [30], could potentially pass through these channels.

To study the route of neuroinvasion after inhalation of RVFV, we sought to visualize RVFV infection of the CNS through the olfactory route. Immunostaining and RNA *in situ* hybridization (ISH) techniques allowed tracking of RVFV from the nasal epithelium, along the ORNs, across the cribriform plate, and into the OB. This study provides foundational

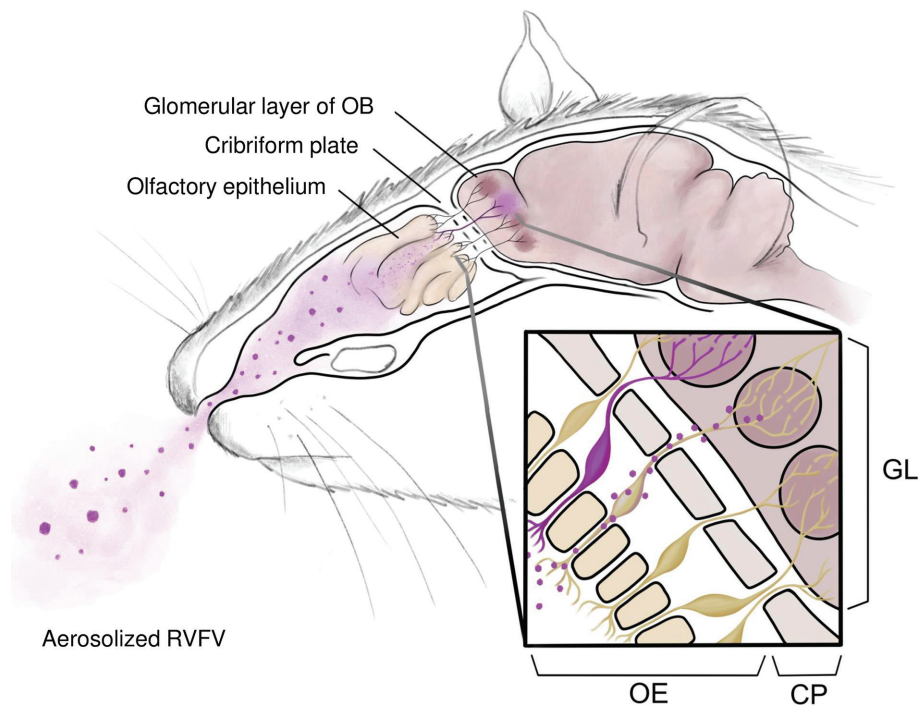


Fig. 1. Structure of the rat nasal passages and proposed pathway of aerosolized Rift Valley fever virus neuroinvasion. Inhaled particles contact the olfactory epithelium (OE), which contains dendritic processes from olfactory receptor neurons (ORNs). Axonal projections from ORNs extend through channels in the cribriform plate (CP) and into the glomerular layer (GL) of the olfactory bulb (OB). Zoom box: RVFV-infected ORNs (purple) or virus associated with ORNs (purple dots) crossing the cribriform plate to gain access to the neuron bundles in the glomerular layer of the olfactory bulb.

information on the olfactory route for neuroinvasion by RVFV after aerosol infection.

METHODS

Biosafety

All work with infectious RVFV (strain ZH501) was performed at biosafety level 3 (BSL-3) in the Regional Biocontainment Laboratory (RBL) at the University of Pittsburgh Center for Vaccine Research. Personnel wore powered air purifying respirators (PAPRs), waterproof gowns, two pairs of gloves and facility-designated scrubs and shoes. Work was conducted in a class III biosafety cabinet (BSC) using Vesphene IIse (Steris Corporation) at a 1:128 working dilution as a disinfectant. All tissues or samples removed from BSL-3 were inactivated using the methods described below; all inactivation methods were verified and approved by University of Pittsburgh biosafety oversight committees. The authors are approved for work with RVFV by the Federal Select Agent Program (FSAP).

Virus propagation

The ZH501 strain of RVFV used in these experiments was generated by reverse genetics and provided by Barry Miller (CDC, Fort Collins, CO, USA) and Stuart Nichol (CDC, Atlanta, GA, USA). Virus was propagated from VERO E6 (CRL-1586, American Type Culture Collection) cells in standard culture conditions using Dulbecco's modified Eagle's medium (DMEM) containing 2% (D2) or 10% (D10) foetal bovine serum (FBS), 1% penicillin/streptomycin (pen/strep) and 1% L-glutamine.

Animal infections

Female Lewis rats (8–10 weeks of age; Envigo) were infected with RVFV ZH501 by aerosol inhalation as described previously [31], with a presented dose of 3×10^4 plaque-forming units (p.f.u.) per rat. Three rats were euthanized at 2, 5 and 7 days p.i. to collect olfactory tissues. Uninfected control rats were similarly euthanized for control tissues. Aerosol infections were performed in a class III aerobiology cabinet as described elsewhere [31].

Whole-head tissue preparation

Rats were perfused with 500 ml of 4% methanol-free paraformaldehyde (PFA) following euthanasia to ensure complete inactivation of tissues in the entire animal. Heads were removed and submerged in fresh 4% PFA and stored at 4°C for fixation for at least 1 week before removal from BSL-3 conditions according to approved inactivation protocols. Decalcification of samples was accomplished by submersion in 10% ethylenediaminetetraacetic acid (EDTA) (pH 7.4) for 3 weeks; each week the sample was moved to a container of fresh EDTA. Decalcification with EDTA is gentle on tissues, preserves DNA and is ideal for use with immunofluorescence [32]. After decalcification, the heads were washed with 1× phosphate-buffered saline (PBS) and placed in 70% ethanol for transport to the University of Pittsburgh McGowan

Institute Histology Core for paraffin embedding and sagittal sectioning

Fluorescence and colorimetric *in situ* hybridization and histology

Whole-snout slides sectioned at a thickness of 8 µm were deparaffinized using an alcohol dehydration series (100, 95 and 70%; each step was repeated twice using fresh reagents and a 10 min incubation time). Slides underwent an antigen retrieval process by boiling in the RNAscope Antigen Retrieval Reagent for 15 min to unmask antigen and probe-binding epitopes. Slides for fluorescent imaging were permeabilized for 30 min using 0.1% TritonX-100 detergent+1× PBS at room temperature (RT) (the RNAscope protease reagent step was omitted to prevent degradation of neuronal structure); colorimetric slides followed the RNAscope 2.5 HD Red detection kit procedure according to the manufacturer's instructions with RVFV ZH501 probe against the NP gene (Advanced Cell Diagnostics cat no. 496931). Slides were stained in a slide box lined with wet paper towels and placed in an incubator at 37°C. Fluorescent samples were stained with Neurotrace-640 (Thermo Fisher Scientific; 1:100 for 1 h at RT) to visualize neuronal bodies, counterstained with Hoescht, and mounted using a glycerol and polyvinyl alcohol (PVA) mixture. Colorimetric slides were counterstained with haematoxylin and mounted using Permount (Fisher Chemical). Deparaffinized slides for pathology observation followed a standard haematoxylin and eosin (H and E) staining procedure. Each staining procedure was completed on five sets of snouts, which included uninfected samples and 2, 5 and 7 days p.i. samples.

Microscopy

Fluorescent ISH slides were imaged using the Nikon A1 confocal microscope provided by the University of Pittsburgh Center for Biologic Imaging, denoised using Nikon Elements software, and contrasted using Adobe Photoshop Elements. Colorimetric ISH slides were imaged using the Zeiss Tissue Gnostics pathology microscope provided by the Center for Biologic Imaging and white balanced using Adobe Photoshop. Pathology slides were imaged using an Olympus CX41 microscope with the Levenhuk M300 base attachment.

RESULTS

Inhalational exposure to RVFV causes extensive infection of the olfactory epithelium

Our previous study found that RVFV vRNA was detectable in the OB as early as 1–2 days p.i., depending upon exposure dose [19, 20]. This finding suggests that the olfactory region plays a part in CNS infection, as the virus encounters the respiratory and olfactory epithelium during inhalation. To study the route of neuroinvasion of RVFV after inhalation exposure, adult female Lewis rats (8–10 weeks old) were exposed to small-particle aerosols of RVFV as described previously [19]. The inhaled dose was 3400 p.f.u., which, based on our previous work, is approximately 34× the LD₅₀.

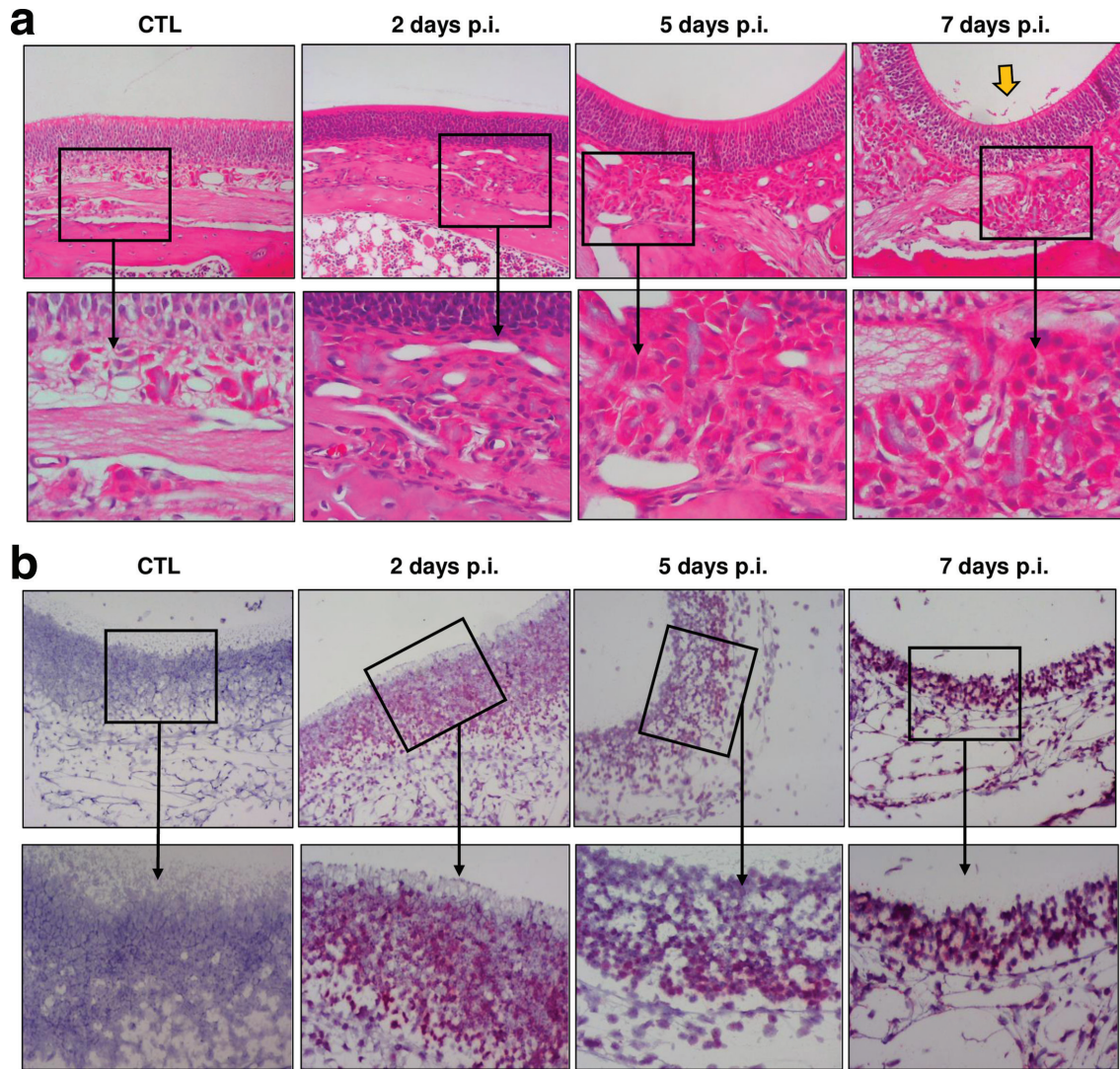


Fig. 2. Extensive infection of the olfactory epithelium by RVFV. (a) H&E tissues at each indicated time point imaged at 10× magnification (top row) with corresponding 20× zoom boxes (bottom row). Yellow arrow indicates cilia sloughing at 7 days p.i. (b) 10× images of RNA ISH (top row) with 20× zoom boxes (bottom row). CTL represents tissue from uninfected control animals. Images shown are representative of $n=3$ at each time point.

At 2, 5 and 7 days p.i., three rats were euthanized on each day, perfused with 4% PFA, and whole heads were decalcified and processed for staining.

Whole rat heads with olfactory region intact were stained with H&E to detect morphological changes within the olfactory tract. The OE remained largely intact and undamaged until 7 days p.i., when cilia sloughing was observed (Fig. 2a, yellow arrow). Extensive detection of vRNA by ISH was observed in OE as early as 2 days p.i., including sustentacular cells and ORNs residing just beneath the epithelial layer (Fig. 2b). This finding suggests that RVFV does not directly damage the OE upon viral infection, yet this region is densely populated with virus-infected cells following inhalational exposure.

Infected cells are found in the cribriform plate soon after exposure

The cribriform plate is a bony structure that serves as a barrier between the nasal turbinate and brain, with small channels allowing for the passage of ORN axons from the OE into the OB (Fig. 1). These channels are essential for relaying olfactory signals from the OE to the CNS via axonal processes. Cribriform plate channels can also be exploited by pathogens and/or particulates as an entry point for access to the OB. H&E staining of the cribriform plate revealed increased cellularity in the lamina propria that lies between it and the OE (Fig. 3a, arrows). Cells within the channels of the cribriform plate stained positive for vRNA at 2 days p.i., which is evidence that this region is highly

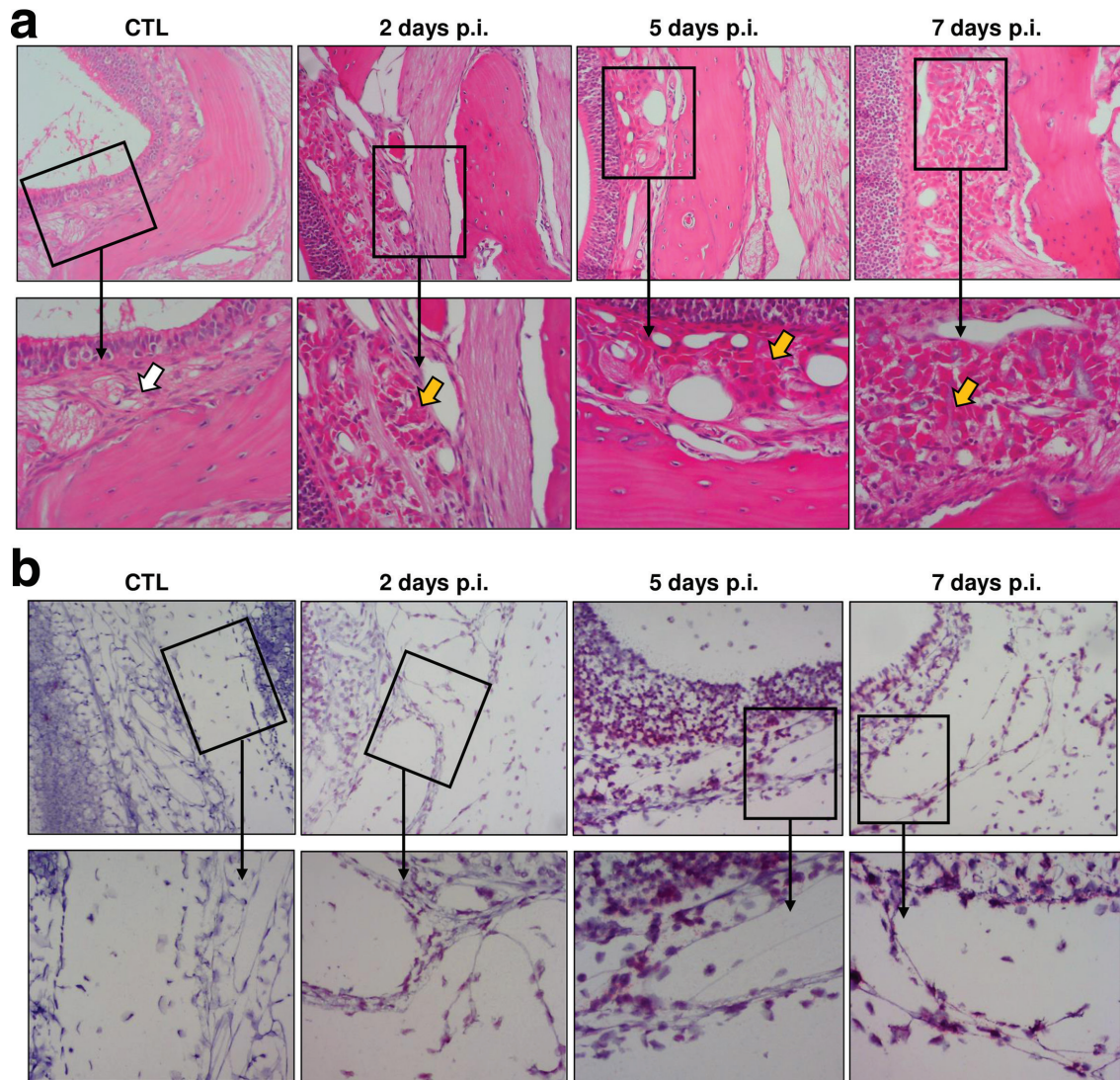


Fig. 3. RVFV infection of cells across the cribriform plate. (a) H&E tissues at each indicated time point imaged at 10× magnification (top row) with corresponding 20× zoom boxes (bottom row). White arrow indicates lamina propria in uninfected control; yellow arrows indicate increased cellularity of this region after RVFV infection. (b) 10× images of RNA ISH (top row) with 20× zoom boxes (bottom row). CTL represents tissue from uninfected control animal. Images shown are representative of $n=3$ at each time point.

infected and likely plays an important role in viral infection of the CNS (Fig. 3b).

Structural integrity of the glomerular layer is lost as infection progresses

The glomerular layer (GL) of the OB is the destination for ORN axons after crossing the cribriform plate (Fig. 1). Healthy normal GL structure is visible by distinct circular structures containing the connections between the termini of the ORN axons and the dendrites of heterogeneous neuronal and glial populations surrounding the glomerulus (Fig. 4a; CTL panels). Periglomerular (PG) neurons form the circular structure that is distinctly visible (Fig. 4a, white arrows). The ORN axons meet groups of neurons in each glomerulus to relay the acquired signals to the rest of the

brain. RVFV infection results in distinct morphological and structural damage in the GL, such as haemorrhage, neuronal loss and major disruption of the GL architecture (Fig. 4; 7 days p.i.) [19]. PG neurons positive for vRNA are visible at 2 and 5 days p.i., with some morphological changes in PG neuronal soma at 5 days p.i. (Fig. 4, green and yellow arrows). By 7 days p.i., the distinct boundaries of the GL become disrupted, eliminating the defined borders separating it from other layers of the OB, and the PG neurons are unhealthy with pyknotic appearance (Fig. 4, blue arrows). This structural loss of neurons and change in GL morphology coincides with the increase in vRNA visualized with ISH (Fig. 4b), as well as clinical signs of neurological distress [19].

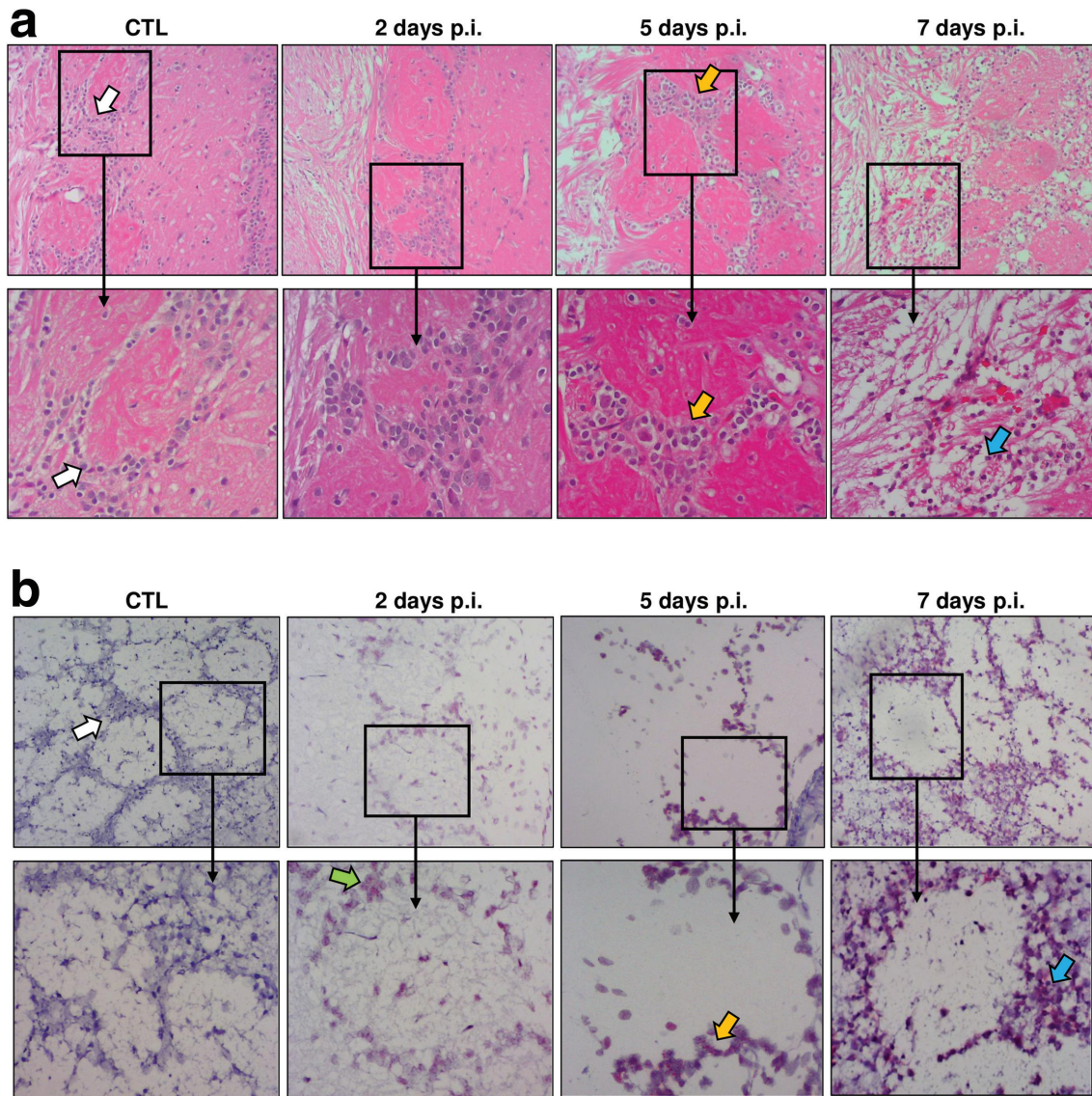


Fig. 4. Loss of integrity in the glomerular layer of the olfactory bulb as RVFV infection progresses. (a) H&E tissues at each indicated time point imaged at 10 \times magnification (top row) with corresponding 20 \times zoom boxes (bottom row). Arrows highlight periglomerular (PG) neurons forming the visible circular structure of the glomeruli. The 20 \times zoom box for 7 days p.i. highlights haemorrhaging. (b) Images of RNA ISH at 10 \times magnification (top row) with 20 \times zoom boxes (bottom row). In uninfected animals (CTL), the glomerular layer (GL) is intact, and healthy PG neurons are visible (white arrows). Infected PG neurons are visible at 2 days p.i. (green arrows). By 5 days p.i., the GL remains intact but PG neurons have an unhealthy appearance, concomitant with viral ISH staining (yellow arrows). By 7 days p.i., GL structure is disrupted and PG neurons are highly infected and pyknotic (blue arrows). Images shown are representative of $n=3$ at each time point.

Inhalational exposure results in rapid infection of the olfactory bulb through the cribriform plate

If RVFV can either infect ORNs or travel along them without directly infecting them, then this could account for the rapid viral invasion in the CNS after inhalational exposure. To obtain an overview of RVFV infection of the OE–OB axis early after infection, whole rat snouts were stained for RVFV vRNA by ISH along with the neuronal

body dye neurotrace (Fig. 5). At 2 days p.i., RVFV-infected cells were visualized within the OE and the lamina propria, and along axons crossing over the cribriform and into the OB (Fig. 5a). Within the cribriform plate at 2 days p.i., RVFV vRNA, neurotrace and DAPI colocalized (visible by pink/orange cells), which supports the hypothesized association between RVFV and the axons of the ORNs crossing through (Fig. 5b, middle panel). A high frequency of PG

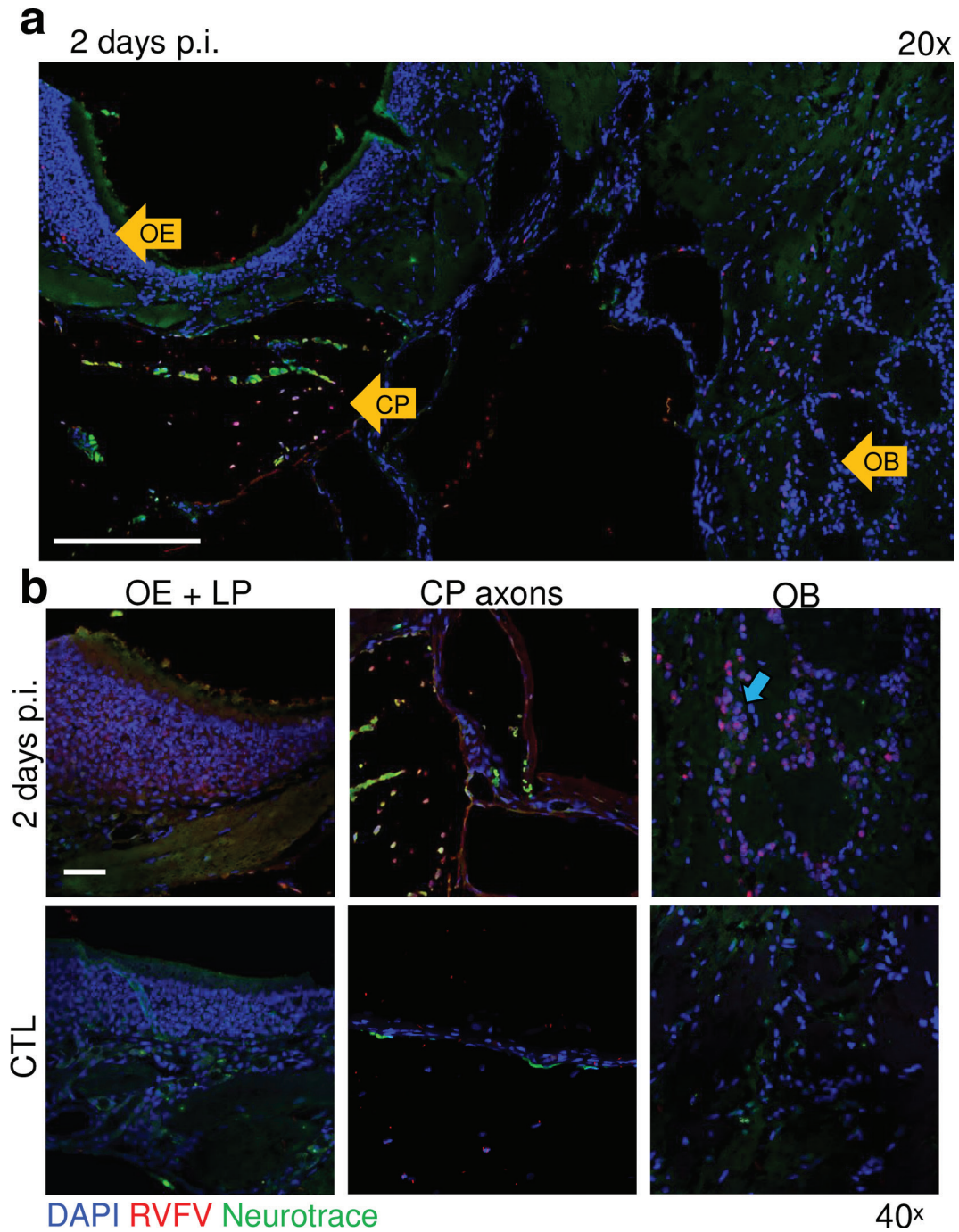


Fig. 5. RVFV-infected cells throughout the olfactory route and olfactory bulb at 2 days p.i. (a) Image (20×) of rat snout/brain at 2 days p.i.: vRNA (red), neurons (green), nuclei (blue). Scale, 250 μm. (b) Micrographs (40×) of relevant structures highlighted by yellow arrows. Blue arrow highlights infected periglomerular (PG) neurons forming the glomeruli. CP, cribriform plate; LP, lamina propria; OB, olfactory bulb. Scale, 50 μm.

neurons in the glomerulus of the OB also stained positive for vRNA at 2 days p.i. (Fig. 5b, blue arrow).

DISCUSSION

While mosquitos facilitate the infection and spread of RVFV between livestock, wild ruminants and humans, exposure to aerosolized RVFV has been documented. For example, abattoir workers inhale aerosolized virions during butchering of infected livestock [33–35]. Cases of respiratory exposure to RVFV have occurred among laboratory workers and in some natural outbreaks [36]; however, there is a lack of epidemiological data to directly link exposure route with severe disease outcomes. The infectiousness of RVFV by aerosol requires it to be studied within BSL-3 containment requirements, under negative pressure, and while using powered air purifying respirators (PAPRs). Aerosol exposure may be associated with a higher risk of severe human disease outcomes such as meningoencephalitis or ocular disease [5, 6, 8]. Aerosol infection studies in rats [19, 20, 31, 37], mice [16–18] and non-human primates (NHPs) [12–14, 38] result in encephalitis and higher mortality rates after aerosol infection than other exposure routes. Additional research into the effects of aerosolized RVFV is crucial because of its environmental stability and ability to be infectious via inhalation [39–41].

A large case study of 683 individuals with laboratory-confirmed RVF during the Saudi outbreak in 2000 identified the most common symptoms as fever (93%), CNS manifestations (17%), haemorrhagic manifestations (7%) and vision loss (2%) [5]. Of the 81 individuals with CNS involvement, symptoms included confusion, lethargy, disorientation, vertigo, coma, tremors and amnesia. Individuals with CNS manifestations were 14.2 times more likely to die than those without a neurological component [5]. While human autopsy specimens are difficult to obtain, a RVFV-seropositive individual who succumbed to meningoencephalitis showed pathological signs of perivascular cuffing and round-cell infiltration [21]. Similar lesions are also seen in the brains of NHPs exposed to aerosolized RVF [12].

Animal models of encephalitic RVF are crucial research tools for illuminating the mechanism of infection that separates cases of self-limiting febrile disease from severe CNS outcomes. When exposed to infectious aerosols of RVFV, Lewis rats develop lethal encephalitis within 7–8 days [31], and we have previously used this model to dissect the neuropathogenic mechanisms of RVFV infection [19, 20, 31, 42]. Our previous work illustrated the temporal spread of leukocyte infiltration and virus replication within the brain of infected rats; however, a major unknown has been the timing and route of entry of RVFV into the CNS after aerosol infection. This study was designed to address this gap in knowledge by visualizing the entire nasal olfactory route from snout to brain after RVFV infection. We optimized several techniques to accomplish this, including proper fixation, decalcification, staining and visualization of viral infection and structural markers.

The structure of the olfactory region in rats is illustrated in Fig. 1. It should be noted that the nasal cavities of human and rodents differ. Human nasal turbinates are relatively simple and prioritize breathing, while rodent nasal turbinates fold and branch in a complex manner that prioritizes olfaction and protection of the lower respiratory tract [43]. In order to support this acute olfaction, rodents have a larger surface area of OE than primates (4 and 1.25%, respectively [44, 45]). In both rodents and primates, ORN bodies reside within the OE, with dendrites that extend down into the OE surface. In humans, the axons of over 10 million ORNs in the OE extend up into the lamina propria, across the cribriform plate, and into the OB. The GL of the OB is the point of attachment of ORN axons into the brain. Glial ensheathing cells support the axons of ORNs as they cross the cribriform plate. These ensheathing cells form fluid-filled channels that remain open and accessible to pathogens, even after ORNs degrade from age. Viral pathogens (influenza viruses [46], herpesviruses [47] and poliovirus [28, 48]) are suspected to use the olfactory route for CNS entry in rodents, NHPs and humans. La Crosse virus, another bunyavirus, was also found to use the olfactory route to enter the brain in mouse models [25].

The severity of RVFV infection in the rat model was evident based on the abundance of infected cells within the OE, the cribriform plate and the glomeruli of the OB by 2 days p.i. Of note is the finding that the OE shows little to no structural damage, unlike what is seen with other neuro-invasive pathogens, such as *Neisseria meningitidis* [49], *Listeria monocytogenes* [50], vesicular stomatitis virus [51], influenza [46] and coronaviruses such as severe acute respiratory syndrome coronavirus 2 (SARS-CoV-2) [52]. We noted only minor sloughing of the cilia late in infection when the animals display clinical signs and have massive leucocyte inflammation and tissue damage in the CNS [19].

ORNs have the ability to uptake exogenous materials and transynaptically transport them to the rest of the CNS; therefore utilization of these neurons could allow RVFV access to the rest of the brain [53]. Additionally, because the OB forms direct connections with the frontal cortex and bypasses the thymus, olfactory pathways do not undergo the antigen processing that the other sensory modalities experience [53]. The rapid appearance of infection in the OB supports the hypothesis that initial viral entry of the CNS is likely due to viral infection traversing the cribriform plate into the OB. Indeed, using immunofluorescent microscopy, we found ORN axons within the cribriform plate area colocalized with vRNA and Neurotrace at 2 days p.i. The staining used in this study cannot conclusively determine whether virus directly infects ORNs or travels through neuron unsheathing cell channels. Bunyaviruses are small (>100 nm) and could fit into these channels, which leaves the possibility for RVFV virions to enter the brain without directly infecting ORNs [54]. However, the extensive vRNA staining of cells within the OE suggests that it is highly likely that the ORNs are directly infected.

Although there are notable structural differences between the nasal mucosa of rodents and humans, the observations made in this study can help illuminate the mechanism of infection that separates disease outcome severity between subcutaneous and inhalational or intranasal exposure to RVFV. In cases of neurological involvement, RVFV leads to long-term morbidity and even death in affected individuals, and there are no current therapeutics to mitigate this disease manifestation. A more thorough understanding of potential neuroinvasion pathways can support the design of more effective therapeutic regimens.

Funding information

Funding was provided by NIH/NINDS R01NS101100 and R21NS088326 to A. L. H. C. M. M. was supported by NIH T32 AI060525.

Acknowledgements

The authors thank Stacey Barrick for coordinating shipment and housing of the animals used in this study and Hayley Nordstrom for illustrating the graphic in Fig. 1.

Conflicts of interest

The authors declare that there are no conflicts of interest.

Ethical statement

This work was approved by the University of Pittsburgh Institutional Animal Care and Use Committee (IACUC) under protocol #17040334. All animal work was conducted in accordance with the recommendations in the Guide for the Care and Use of Laboratory Animals of the National Resource Council. All animals were housed and fed in an Association for Assessment and Accreditation of Laboratory Animal Care accredited facility. Euthanasia criteria were based on fever, weight loss and morbidity, and were approved by the IACUC.

References

- Davies FG, Martin V. Recognizing Rift Valley Fever. FAO Animal Health manual Food and Agriculture Organization of the United Nations. Volume 17. Available at: <http://www.fao.org/3/y4611e/y4611e00.htm> 2003.
- McIntosh BM, Russell D, dos Santos I, Gear JH. Rift Valley fever in humans in South Africa. *S Afr Med J* 1980;58:803–806.
- Al-Hazmi A, Al-Rajhi AA, Abboud EB, Ayoola EA, Al-Hazmi M et al. Ocular complications of Rift Valley fever outbreak in Saudi Arabia. *Ophthalmology* 2005;112:313–318.
- Laughlin LW, Meegan JM, Strausbaugh LJ, Morens DM, Watten RH. Epidemic Rift Valley fever in Egypt: observations of the spectrum of human illness. *Trans R Soc Trop Med Hyg* 1979;73:630–633.
- Madani TA, Al-Mazrou YY, Al-Jeffri MH, Mishkhas AA, Al-Rabeah AM et al. Rift Valley fever epidemic in Saudi Arabia: epidemiological, clinical, and laboratory characteristics. *Clin Infect Dis* 2003;37:1084–1092.
- Strausbaugh LJ, Laughlin LW, Meegan JM, Watten RH. Clinical studies on Rift Valley fever, part I: acute febrile and hemorrhagic-like diseases. *J Egypt Public Health Assoc* 1978;53:181–182.
- Abdel-Wahab KS, El Baz LM, El-Tayeb EM, Omar H, Ossman MA et al. Rift Valley fever virus infections in Egypt: pathological and virological findings in man. *Trans R Soc Trop Med Hyg* 1978;72:392–396.
- LaBeaud AD, Pfeil S, Muiruri S, Dahir S, Sutherland LJ et al. Factors associated with severe human Rift Valley fever in Sangailu, Garissa County, Kenya. *PLoS Negl Trop Dis* 2015;9:e0003548.
- Anyangu AS, Gould LH, Sharif SK, Nguku PM, Omolo JO et al. Risk factors for severe Rift Valley fever infection in Kenya, 2007. *Am J Trop Med Hyg* 2010;83:14–21.
- Nicholas DE, Jacobsen KH, Waters NM. Risk factors associated with human Rift Valley fever infection: systematic review and meta-analysis. *Trop Med Int Health* 2014;19:1420–1429.
- Hoogstraal H, Meegan JM, Khalil GM, Adham FK. The Rift Valley fever epizootic in Egypt 1977–78. 2. ecological and entomological studies. *Trans R Soc Trop Med Hyg* 1979;73:624–629.
- Hartman AL, Powell DS, Bethel LM, Caroline AL, Schmid RJ et al. Aerosolized Rift Valley fever virus causes fatal encephalitis in African green monkeys and common marmosets. *J Virol* 2014;88:2235–2245.
- Wonderlich ER, Caroline AL, McMillen CM, Walters AW, Reed DS et al. Peripheral blood biomarkers of disease outcome in a monkey model of Rift Valley fever encephalitis. *J Virol* 2018;92 [Epub ahead of print 01 02 2018].
- Smith DR, Bird BH, Lewis B, Johnston SC, McCarthy S et al. Development of a novel nonhuman primate model for Rift Valley fever. *J Virol* 2012;86:2109–2120.
- Hickerson BT, Westover JB, Van Wettene AJ, Rigas JD, Miao J et al. Pathogenesis of Rift Valley fever virus aerosol infection in STAT2 knockout hamsters. *Viruses* 2018;10:651 [Epub ahead of print 19 11 2018].
- Scharton D, Bailey KW, Vest Z, Westover JB, Kumaki Y et al. Favi-piravir (T-705) protects against peracute Rift Valley fever virus infection and reduces delayed-onset neurologic disease observed with ribavirin treatment. *Antiviral Res* 2014;104:84–92.
- Reed C, Lin K, Wilhelmsen C, Friedrich B, Nalca A et al. Aerosol exposure to Rift Valley fever virus causes earlier and more severe neuropathology in the murine model, which has important implications for therapeutic development. *PLoS Negl Trop Dis* 2013;7:e2156.
- Dodd KA, McElroy AK, Jones TL, Zaki SR, Nichol ST et al. Rift Valley fever virus encephalitis is associated with an ineffective systemic immune response and activated T cell infiltration into the CNS in an immunocompetent mouse model. *PLoS Negl Trop Dis* 2014;8:e2874.
- Albe JR, Boyles DA, Walters AW, Kujawa MR, McMillen CM et al. Neutrophil and macrophage influx into the central nervous system are inflammatory components of lethal Rift Valley fever encephalitis in rats. *PLoS Pathog* 2019;15:e1007833-e.
- Walters AW, Kujawa MR, Albe JR, Reed DS, Klimstra WB et al. Vascular permeability in the brain is a late pathogenic event during Rift Valley fever virus encephalitis in rats. *Virology* 2019;526:173–179.
- van Velden DJ, Meyer JD, Olivier J, Gear JH, McIntosh B. Rift Valley fever affecting humans in South Africa: a clinicopathological study. *S Afr Med J* 1977;51:867–871.
- Esiri MM. Herpes simplex encephalitis: an immunohistological study of the distribution of viral antigen within the brain. *J Neurol Sci* 1982;54:209–226.
- Smith GA, Gross SP, Enquist LW. Herpesviruses use bidirectional fast-axonal transport to spread in sensory neurons. *Proc Natl Acad Sci U S A* 2001;98:3466–3470.
- Munster VJ, Prescott JB, Bushmaker T, Long D, Rosenke R et al. Rapid Nipah virus entry into the central nervous system of hamsters via the olfactory route. *Sci Rep* 2012;2:736.
- Bennett RS, Cress CM, Ward JM, Firestone C-Y, Murphy BR et al. Pathogenesis, and immunogenicity in mice and monkeys. *Virol J* 2008;5:25.
- Casiraghi C, Dorovini-Zis K, Horwitz MS. Epstein-Barr virus infection of human brain microvessel endothelial cells: a novel role in multiple sclerosis. *J Neuroimmunol* 2011;230:173–177.
- Clay CC, Rodrigues DS, Ho YS, Fallert BA, Janatpour K et al. Neuroinvasion of Fluorescein-Positive monocytes in acute simian immunodeficiency virus infection. *J Virol* 2007;81:12040–12048.
- Faber HK, Silverberg RJ, Dong L. Poliomyelitis in the cynomolgus monkey: iii. infection by inhalation of droplet nuclei and the nasopharyngeal portal of entry, with a note on this mode of infection in rhesus. *J Exp Med* 1944;80:39–57.
- Crotty S, Hix L, Sigal LJ, Andino R. Poliovirus pathogenesis in a new poliovirus receptor transgenic mouse model: age-dependent paralysis and a mucosal route of infection. *J Gen Virol* 2002;83:1707–1720.

30. Shope RE. *Bunyaviruses. Medical Microbiology*. Galveston, TX: The University of Texas Medical Branch at Galveston; 1996.
31. Bales JM, Powell DS, Bethel LM, Reed DS, Hartman AL. Choice of inbred rat strain impacts lethality and disease course after respiratory infection with Rift Valley fever virus. *Front Cell Infect Microbiol* 2012;2:105.
32. Alers JC, Krijtenburg P-J, Vissers KJ, van Dekken H. Effect of bone decalcification procedures on DNA in situ hybridization and comparative genomic hybridization: EDTA is highly preferable to a routinely used acid Decalcifier. *J Histochem Cytochem* 1999;47:703–709.
33. Abu-Elyazeed R, el-Sharkawy S, Olson J, Botros B, Soliman A et al. Prevalence of anti-Rift-Valley-fever IgM antibody in abattoir workers in the Nile delta during the 1993 outbreak in Egypt. *Bull World Health Organ* 1996;74:155–158.
34. Turkistany AH, Mohamed AG, Al-Hamdan N. Seroprevalence of Rift Valley fever among slaughterhouse personnel in Makkah during hajj 1419h (1999). *J Fam Community Health* 2001;8:53–57.
35. Chambers PG, Swanepoel R. Rift valley fever in abattoir workers. *Cent Afr J Med* 1980;26:122–126.
36. Smithburn KC, Mahaffy AF, Haddow AJ, Kitchen SF, Smith JF. Rift Valley fever; accidental infections among laboratory workers. *J Immunol* 1949;62:213–227.
37. Caroline AL, Powell DS, Bethel LM, Oury TD, Reed DS et al. Broad spectrum antiviral activity of favipiravir (T-705): protection from highly lethal inhalational Rift Valley fever. *PLoS Negl Trop Dis* 2014;8:e2790.
38. Morrill JC, Jennings GB, Johnson AJ, Cosgriff TM, Gibbs PH et al. Pathogenesis of Rift Valley fever in rhesus monkeys: role of interferon response. *Arch Virol* 1990;110:195–212.
39. Borio L, Inglesby T, Peters CJ, Schmaljohn AL, Hughes JM et al. Hemorrhagic fever viruses as biological weapons: medical and public health management. *JAMA* 2002;287:2391–2405.
40. Miller WS, Demciak P, Rosenberger CR, Dominik JW, Bradshaw JL. Stability and infectivity of airborne yellow fever and Rift Valley fever viruses. *Am J Hyg* 1963;77:114–121.
41. Sidwell RW, Smee DF. Viruses of the Bunya- and Togaviridae families: potential as bioterrorism agents and means of control. *Antiviral Res* 2003;57:101–111.
42. Caroline AL, Kujawa MR, Oury TD, Reed DS, Hartman AL. Inflammatory biomarkers associated with lethal Rift Valley fever encephalitis in the Lewis rat model. *Front Microbiol* 2016;6.
43. Harkema JR, Carey SA, Wagner JG. The nose revisited: a brief review of the comparative structure, function, and toxicologic pathology of the nasal epithelium. *Toxicol Pathol* 2006;34:252–269.
44. Escada P. [Localization and distribution of human olfactory mucosa in the nasal cavities]. *Acta Med Port* 2013;26:200–207.
45. Gross EA, Swenberg JA, Fields S, Popp JA. Comparative morphology of the nasal cavity in rats and mice. *J Anat* 1982;135:83–88.
46. van Riel D, Leijten LM, Verdijk RM, GeurtsvanKessel C, van der Vries E et al. Evidence for influenza virus CNS invasion along the olfactory route in an immunocompromised infant. *J Infect Dis* 2014;210:419–423.
47. Harberts E, Yao K, Wohler JE, Maric D, Ohayon J et al. Human herpesvirus-6 entry into the central nervous system through the olfactory pathway. *Proc Natl Acad Sci U S A* 2011;108:13734–13739.
48. Faber HK, Silverberg RJ. A neuropathological study of acute human Polio-myelitis with special reference to the initial lesion and to various potential portals of entry. *J Exp Med* 1946;83:329–353.
49. Sjölander H, Jonsson A-B. Olfactory nerve—a novel invasion route of *Neisseria meningitidis* to reach the meninges. *PLoS One* 2010;5:e14034-e.
50. Pägelow D, Chhatbar C, Beineke A, Liu X, Nerlich A et al. The olfactory epithelium as a port of entry in neonatal neuroinfection. *Nat Commun* 2018;9:4269.
51. Moseman EA. Mucosal immune mediated protection of the CNS following olfactory viral infection. *J Immunol Res* 2019;202:66.7–7.
52. Soler ZM, Patel ZM, Turner JH, Holbrook EH. A primer on viral-associated olfactory loss in the era of COVID-19. *Int Forum Allergy Rhinol* 2020;10:814–820.
53. Mori I, Nishiyama Y, Yokochi T, Kimura Y. Olfactory transmission of neurotropic viruses. *J Neuroviral* 2005;11:129–137.
54. Williams SK, Franklin RJM, Barnett SC. Response of olfactory ensheathing cells to the degeneration and regeneration of the peripheral olfactory system and the involvement of the neuregulins. *J Comp Neurol* 2004;470:50–62.

Five reasons to publish your next article with a Microbiology Society journal

1. The Microbiology Society is a not-for-profit organization.
2. We offer fast and rigorous peer review – average time to first decision is 4–6 weeks.
3. Our journals have a global readership with subscriptions held in research institutions around the world.
4. 80% of our authors rate our submission process as 'excellent' or 'very good'.
5. Your article will be published on an interactive journal platform with advanced metrics.

Find out more and submit your article at microbiologyresearch.org.